Med Chem Res
DOI 10.1007/s00044-017-2090-8

MEDICINAL CHEMISTRY RESEARCH

ORIGINAL RESEARCH

Newer series of trioxane derivatives as potent antimalarial agents

Mithun Rudrapal[1] · **Zartaj Washmin Banu**[1] · **Dipak Chetia**[1]

Received: 13 June 2017 / Accepted: 25 September 2017

Abstract Among synthesized 1,2,4-trioxane derivatives, six compounds were found to be considerably potent, with better activity against resistant strain of *P. falciparum* than the sensitive strain. The IC_{50} values of the best compound with 4-hydroxyphenyl substitution were found to be 0.391 and 0.837 µg/mL against sensitive and resistant strain of *P. falciparum*, respectively. Results of the tested compounds were comparable with that of the standard drug, chloroquine ($IC_{50} = 0.044$ and 0.205 µg/mL against sensitive and resistant strain of *P. falciparum*, respectively). Docking simulation, in silico drug-likeness and ADMET studies further validated the results of in vitro antimalarial activity. Trioxane derivatives exhibited good binding affinity for the *P. falciparum* cysteine protease falcipain 2 receptor (PDB id: 3BPF) with well defined drug-like and pharmacokinetic properties based on Lipinski's rule of five with additional physicochemical and ADMET parameters. In view of having antimalarial potential, newly reported 1,2,4-trioxane derivative(s) may be useful as novel antimalarial lead(s) in the discovery and development of future antimalarial drug candidates as *P. falciparum* falcipain 2 inhibitors against resistant malaria.

Keywords *P. falciparum* · Resistance · 1,2,4-Trioxane · Falcipain 2 inhibitors · Antimalarial

✉ Mithun Rudrapal
rudrapal.m03@gmail.com

[1] Department of Pharmaceutical Sciences, Dibrugarh University, Dibrugarh 786 004 Assam, India

Introduction

Malaria continues to be a major lethal infectious disease of human beings, affecting around 200–300 million people and causing approximately 430,000 deaths every year globally (WHO 2016). *Plasmodium falciparum* is the most prevalent and deadly species that causes severe malaria such as cerebral malaria, and it is also responsible for most of the malaria-related deaths in humans (Rudrapal and Chetia 2016; Pandey et al. 2013; Gogoi et al. 2016). Every year over 50% of all malarial infections are caused by *P. falciparum* with about 20–50% of total mortality cases, particularly in children younger than 5 years old and pregnant women (Geleta and Ketema 2016). During the past two decades, the emergence of drug resistant strains of *P. falciparum* has become an increasingly serious concern in malaria control and prevention worldwide (Rudrapal and Chetia 2016). Artemisinin (ART)-based combination therapies (ACTs) such as artemether + lumefantrine + amodiaquine and artesunate + mefloquine + piperaquine recommended by WHO for the treatment of multi-drug resistant *P. falciparum* malaria have also been reported to develop resistance in some parts of the world (Rudrapal and Chetia 2016; Kyle et al. 1998). This increasing burden of resistant malaria has stimulated drug discovery scientists to search for new antimalarial drugs or alternative therapeutic options to combat the problem of drug resistance. In view of this, the development of new antimalarial drugs with novel mode(s) of action could be an attractive strategy to address the above challenging issue. In recent years, research into several synthetic endoperoxide scaffolds such as 1,2,4-trioxane, 1,2,4-trioxolane and 1,2,4,5-teraoxane derivatives and their hybrid analogs have gained significant interest in discovery and development of potent antimalarial drugs. Some endoperoxide-based antimalarial compounds

Published online: 03 October 2017

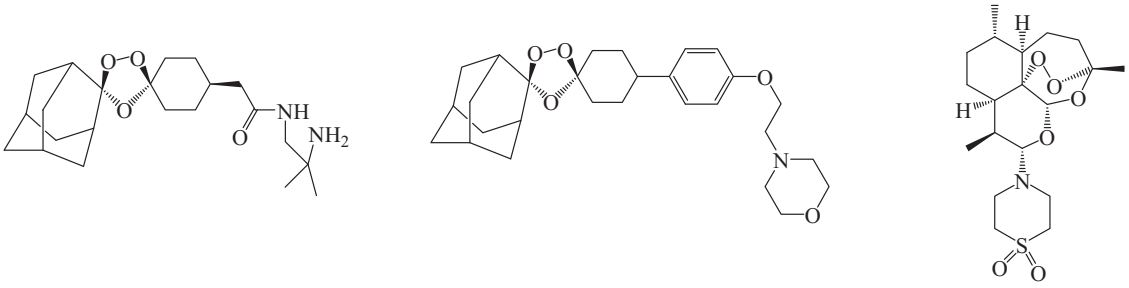

OZ 277 (Arterolane) OZ 439 (Artefenomel) BAY 44 9585 (Artemisone)

Fig. 1 Structures of some endoperoxide antimalarials under clinical development

(Rudrapal and Chetia 2016) that are currently under clinical phase of development are represented in Fig. 1. Endoperoxide molecules bearing 1,2,4-trioxane core have been identified to exhibit a broad spectrum of biological effects such as anticancer, antimicrobial, and anti-parasitic effects (Rubush et al. 2012). Several design strategies have been initiated by medicines for malaria venture (MMV) program for the development of effective and affordable synthetic peroxides as alternative therapy to existing ART-based drugs (Rudrapal and Chetia 2016; Tang et al. 2004). However, considering all above facts, development of peroxide-based synthetic compounds is expected provide effective antimalarials agents with limited toxicity issues and ready to be available at affordable cost. It would offer a better therapeutic option for the treatment of malaria with good clinical outcomes (desired potency with optimal pharmacokinetics) and resistant preventing action over ART, its semi-synthetic analogs and related endoperoxides. It may therefore represent a new class of synthetic, new-generation, and orally active peroxides, with optimal antimalarial potency against resistant *P. falciparum* malaria.

As part of our research program towards developing potent antimalarial drugs that would be active against resistant *P. falciparum* malaria, novel molecular manipulation approach was adopted to design and develop newer series of 1,2,4-trioxane derivatives as single drug conjugates (single molecular entity rather than hybrid drugs) based on the basic structural scaffold of 1,2,4-trioxane ring system. After the synthesis of compounds, in vitro antimalarial screening, molecular docking and drug-likeness studies including ADMET prediction using in silico tools were also carried out. Since, ART and its semi-synthetic analogs or ART derived peroxides possess unfavorable pharmacokinetic issues and certain tissue toxicities because of their high structural complexities and some physicochemical insufficiencies (Garner and Graves 2005; Park et al. 1998), it is expected that designed compounds would possess modified pharmacokinetic properties and toxicities due to less complexities in the molecular structure. Moreover, single drug conjugate-based trioxane molecule can be given as single drug therapy that would also be advantageous over hybrid antimalarial drugs and combination therapies.

Molecular docking study was performed to validate the antimalarial efficacy of synthesized 1,2,4-trioxane derivatives by investigating binding modes as well as orientation of ligands in the receptor pocket of target falcipain 2 protein (*P. falciparum* cysteine protease enzyme). In our study, three dimensional structure of falcipain 2 protein molecule was used as possible antimalarial drug target for 1,2,4-trioxane derivatives. Docking rationalizes finding new antimalarial lead molecules and also gives an insight into structure-activity relationships and mode(s) of antimalarial action based on scoring function and further binding modes analysis from ligand-protein binding/interaction studies (Singh and Konwar 2012). Drug-likeness study includes calculation of fundamental molecular (physicochemical) properties and Lipinski's parameters, which assesses the acceptability of compounds as drug molecules. They represent the combined physicochemical, pharmacokinetic, and pharmacodynamic properties (collectively termed as drug-like properties) of molecules to exhibit good drug-likeness behavior in human body (Shukla et al. 2013). In fact, molecular properties are the fundamental structural parameters which determine the physicochemical (solubility and permeability) and biochemical (metabolic stability, transport property, and protein/tissue affinity) properties, which ultimately determine molecule's in vivo pharmacokinetics (bioavailability and half life), toxicity and pharmacodynamics (receptor affinity and efficacy) (Sharma et al. 2016) ADMET (absorption, distribution, metabolism, excretion, and toxicity) properties have a predictable influence on pharmacokinetic and pharmacodynamic effects of drug molecules. The calculation of ADMET properties is therefore intended as the first step towards optimizing the new drug molecules, whether to check the failure of lead molecules which may cause toxicity and one unable to cross the intestinal membranes or metabolized by the body in to an inactive form (Singh and Srivastava 2015).

Experimental

Synthesis and analysis

All of the chemicals were procured commercially from Sigma-Aldrich Corporation (USA), Merck Specialists Pvt. Ltd. (Germany), HiMedia Lab. Pvt. Ltd. (Germany) or Spectrochem Pvt. Ltd. (India) and were used without further purification. All the reactions were performed in oven dried glass ware using synthetic grade chemicals. Melting points (MP) were measured in open capillaries on an electrically heated melting point apparatus. Ultraviolet (UV)–Visible spectra were recorded on Shimadzu UV-1700 UV–Visible spectrophotometer and the wave lengths of maximum absorption (λ_{max}, nm) are reported. Infrared (IR) spectra were obtained on a Bruker Alpha Fourier transform (FT-IR) spectrometer using KBr disc and are reported in terms of frequency of absorption (υ, cm^{-1}). ^{1}H & ^{13}C nuclear magnetic resonance (NMR) spectra were recorded on Bruker Avance II 400 FT-NMR spectrometer at 400 and 100 MHz, respectively using tetramethylsilane (TMS) as an internal standard (δ 0.00 ppm) and $CDCl_3$ as a solvent. Chemical shift (δ) values were expressed in parts per million (ppm) relative to TMS (δ 0.00 ppm). ^{1}HNMR data are assigned in order: peak multiplicity (s, singlet; d, doublet; t, triplet; m, multiplet), number of protons (numerical integral value), coupling constants (J value) in hertz. ^{13}C NMR data represents different types of structural carbons with respect to their corresponding chemical shift values. Mass spectra were obtained on a LC–MS Water 4000 ZQ instrument using electrospray ionization. The *m/z* values were recorded in the range of *m/z* between 100–500 and the *m/z* values of the most intense molecular ion $[M]^+$ peak, with relative intensities in parentheses, are given followed by peaks corresponding to major fragment ions.

General procedure of synthesis 3a–j

A mixture of *p*-cresol, **1** (1 mmol, 0.1045 mL), distilled water (16.0 mL) and acetonitrile (CH_3CN, 4.0 mL) was vigorously stirred until complete solution was achieved. A mixture of oxone (5 mmol, 1.537 g) and $NaHCO_3$ (15 mmol, 1.261 g), previously ground into powder, was slowly added in portion, and a septum with an empty balloon was immediately placed into the flask in order to avoid over-pressure and loss of generated singlet oxygen. The mixture was vigorously stirred at room temperature until total disappearance of the phenol. After about 1 h of stirring, the reaction was quenched with water and extracted several times (3–4 times) with ethyl acetate (EtOAc). Combined ethyl acetate extracts were dried in Na_2SO_4 and the solvent was removed under reduced pressure to yield the product of *p*-peroxyquinol, **2**. The crude compound was recrystallized from ethyl acetate/ethanol mixture (3:1) to obtain a pure product of white crystalline solid.

The intermediate compound, *p*-peroxiquinol (4-methyl-4-hydroperoxycyclohexa-2,5-dienone) **2** (1 mmol) was added slowly into a mixture of aldehyde (1.5 mmol) and dichloromethane (4.0 mL), followed by the addition of an acid catalyst, *p*-toluenesulfonic acid (PTSA, 0.05 mmol). The reaction mixture was stirred at 45–50 °C till the completion of reaction (8–12 h) and then concentrated in vacuum. Solvent recrystallization of the resulting residue with ethanol the desired pure product of target compounds, **3a–j** as crystalline solids or semi-solids (Rubush et al. 2012; Carreno et al. 2006).

*8a-methyl-4a,5-dihydrobenzo-1,2,4-trioxin-6(8aH)-one (**3a**)*

UV spectrum (MeOH), λ_{max}, nm: 202.5; IR (KBr, cm^{-1}) *υ*: 2932.02, 2894.01 (C–H, CH_3), 1656.48 (C=O, conj.), 1145.20 (C–O), 892.28 (O–O); ^{1}H NMR (400 MHz, $CDCl_3$) δ: 1.23 (s, 3H, CH_3), 2.46 (d, $J = 3.0$ Hz, 2H, CO–C<u>H</u>$_2$–CH), 4.12 (d, $J = 3.0$ Hz, 1H, CO–CH$_2$–C<u>H</u>), 6.04 (d, $J = 9.0$, 1H, CO–CH=C<u>H</u>), 6.32 (d, $J = 9.0$, 1H, CO–C<u>H</u>=CH); ^{13}C NMR (100 MHz, $CDCl_3$) δ: 18.24 (CH_3), 24.23, 28.78 (CH_2), 36.81, 42.37 (CH), 84.77, 92.40 (CH=CH), 188.27 (C=O); MS (ES^+), *m/z* (%): 170.57 (100), $[M]^+$.

*3-Methyl-8a-methyl-4a,5-dihydrobenzo-1,2,4-trioxin-6 (8aH)-one (**3b**)*

UV spectrum (MeOH), λ_{max}, nm: 212.7; IR (KBr, cm^{-1}) *υ*: 2940.31, 2883.27 (C–H, CH_3), 1643.20 (C=O, conj.), 1145.32 (C–O), 898.20 (O–O); ^{1}H NMR (400 MHz, $CDCl_3$) δ: 0.84 (s, 3H, CH_3), 1.22 (s, 3H, CH_3), 2.48 (d, $J = 3.0$ Hz, 2H, CO–C<u>H</u>$_2$–CH), 4.20 (d, $J = 3.0$ Hz, 1H, CO–CH$_2$–C<u>H</u>), 6.12 (d, $J = 9.0$, 1H, CO–CH=C<u>H</u>), 6.42 (d, $J = 9.0$, 1H, CO–C<u>H</u>=CH); ^{13}C NMR (100 MHz, $CDCl_3$) δ: 14.20, 18.12 (CH_3), 26.23 (CH_2), 36.45, 42.12 (CH), 84.42, 90.20 (CH=CH), 188.19 (C=O); MS (ES^+), *m/z* (%): 184.67 (100), $[M]^+$.

*3-Isopropyl-8a-methyl-4a,5-dihydrobenzo-1,2,4-trioxin-6 (8aH)-one (**3c**)*

UV spectrum (MeOH), λ_{max}, nm: 219.4; IR (KBr, cm^{-1}) *υ*: 2964.42, 2884.03 (C–H, CH_3), 1666.23 (C=O, conj.), 1178.23 (C–O), 887.21 (O–O); ^{1}H NMR (400 MHz, $CDCl_3$) δ: 0.82 (s, 3H, CH_3), 1.15 (s, 3H, CH_3), 1.46 (m, 2H, CH$_2$–C<u>H</u>$_2$–CH$_3$), 2.42 (d, $J = 3.0$ Hz, 2H, CO–C<u>H</u>$_2$–CH), 4.26 (d, $J = 3.0$ Hz, 1H, CO–CH$_2$–C<u>H</u>), 4.89 (m, C<u>H</u>(CH$_3$)$_3$), 6.08 (t, $J = 8.0$ Hz, 1H, C<u>H</u>–CH$_2$–CH$_3$), 6.14 (d, $J = 9.0$, 1H, CO–CH=C<u>H</u>), 6.42

(d, $J = 9.0$, 1H, CO–C<u>H</u>=CH); ^{13}C NMR (100 MHz, $CDCl_3$) δ: 15.84, 18.12 (CH_3), 32.20 (CH_2), 34.02, 46.29 (CH), 84.50, 94.02 (CH=CH), 188.12 (C=O); MS (ES^+), *m/z* (%): 212.42 (100), $[M]^+$.

*3-Phenyl-8a-methyl-4a,5-dihydrobenzo-1,2,4-trioxin-6 (8aH)-one (**3d**)*

UV spectrum (MeOH), λ_{max}, nm: 223.0; IR (KBr, cm^{-1}) υ: 3162.24 (O–H, bonded), 2968.00, 2874.10 (C–H, CH_3), 1667.12 (C=O, conj.), 1582.19, 1560.32, 1532.21, 1426.14 (C=C, aryl), 1163.21 (C–O), 836.27 (O–O); ^{1}H NMR (400 MHz, $CDCl_3$) δ: 1.12 (s, 3H, CH_3), 2.42 (d, $J = 8.0$ Hz, 2H, CO–C<u>H</u>$_2$–CH), 4.20 (d, $J = 8.0$ Hz, 1H, CO–CH$_2$–C<u>H</u>), 6.22 (d, $J = 9.0$, 1H, CO–CH=C<u>H</u>), 6.34 (d, $J = 9.0$, 1H, CO–C<u>H</u>=CH), 7.24 (d, $J = 8.0$ Hz, 1H, Ar–H), 7.37 (d, $J = 7.0$ Hz, 1H, Ar–H), 7.81 (d, $J = 8.0$ Hz, 1H, Ar–H); ^{13}C NMR (100 MHz, $CDCl_3$) δ: 15.20 (CH_3), 38.42 (CH), 86.30, 92.77 (CH=CH), 116.11, 130.12, 134.04, 148.55, 156.12, 161.40 (Ar–C), 191.34 (C=O); MS (ES^+), *m/z* (%): 246.42 (100), $[M]^+$.

*3-(3-Hydroxyphenyl)-8a-methyl-4a,5-dihydrobenzo-1,2,4-trioxin-6(8aH)-one (**3e**)*

UV spectrum (MeOH), λ_{max}, nm: 217.5; IR (KBr, cm^{-1}) υ: 3174.10 (O–H, bonded), 2970.21, 2879.23 (C–H, CH_3), 1667.13 (C=O, conj.), 1595.12, 1514.23, 1423.14 (C=C, aryl), 1172.70 (C–O), 832.19 (O–O); ^{1}H NMR (400 MHz, $CDCl_3$) δ: 1.19 (s, 3H, CH_3), 2.42 (d, $J = 3.0$ Hz, 2H, CO–C<u>H</u>$_2$–CH), 4.22 (d, $J = 3.0$ Hz, 1H, CO–CH$_2$–C<u>H</u>), 6.08 (d, $J = 10.0$, 1H, CO–CH=C<u>H</u>), 6.32 (d, $J = 10.0$, 1H, CO–C<u>H</u>=CH), 7.14 (d, $J = 7.0$ Hz, 1H, Ar–H), 7.22 (d, $J = 7.0$ Hz, 1H, Ar–H), 7.48 (d, $J = 8.0$ Hz, 1H, Ar–H), 7.80 (d, $J = 8.0$ Hz, 1H, Ar–<u>H</u>), 9.52 (Ar–OH); ^{13}C NMR (100 MHz, $CDCl_3$) δ: 15.47 (CH_3), 36.42 (CH), 86.20, 96.00 (CH=CH), 118.12, 132.04, 136.24, 140.10, 148.02, 158.12 (Ar–C), 188.24 (C=O); MS (ES^+), *m/z* (%): 262.28 (100), $[M]^+$.

*3-(3,4-Dihydroxyphenyl)-8a-methyl-4a,5-dihydrobenzo-1,2,4-trioxin-6(8aH)-one (**3f**)*

UV spectrum (MeOH), λ_{max}, nm: 254.5; IR (KBr, cm^{-1}) υ: 3182.67 (O–H, bonded), 2970.21, 2879.23 (C–H, CH_3), 1667.13 (C=O, conj.), 1595.12, 1514.23, 1423.14 (C=C, aryl), 1161.15 (C–O), 834.70 (O–O); ^{1}H NMR (400 MHz, $CDCl_3$) δ: 1.18 (s, 3H, CH_3), 2.44 (d, $J = 8.0$ Hz, 2H, CO–C<u>H</u>$_2$–CH), 4.26 (d, $J = 7.0$ Hz, 1H, CO–CH$_2$–C<u>H</u>), 6.07 (d, $J = 10.0$, 1H, CO–CH=C<u>H</u>), 6.22 (d, $J = 10.0$, 1H, CO–C<u>H</u>=CH), 7.42 (d, $J = 8.0$ Hz, 1H, Ar–H), 7.47 (d, $J = 8.0$ Hz, 1H, Ar–H), 7.86 (s, 1H, Ar–<u>H</u>), 9.64 (Ar–OH); ^{13}C NMR (100 MHz, $CDCl_3$) δ: 15.42 (CH_3), 36.70 (CH), 86.10, 94.16 (CH=CH), 116.34, 133.00, 138.14, 142.20, 147.56, 152.02 (Ar–C), 186.37 (C=O); MS (ES^+), *m/z* (%): 278.53 (100), $[M]^+$.

*3-(4-Hydroxyphenyl)-8a-methyl-4a,5-dihydrobenzo-1,2,4-trioxin-6(8aH)-one (**3g**)*

UV spectrum (MeOH), λ_{max}, nm: 229.5; IR (KBr, cm^{-1}) υ: 3186.13 (O–H, bonded), 2968.12, 2882.40 (C–H, CH_3), 1682.45 (C=O, conj.), 1584.00, 1549.12, 1468.45 (C=C, aryl), 1162.30 (C–O), 845.20 (O–O); ^{1}H NMR (400 MHz, $CDCl_3$) δ: 1.22 (s, 3H, CH_3), 2.48 (d, $J = 8.0$ Hz, 2H, CO–C<u>H</u>$_2$–CH), 4.24 (d, $J = 8.0$ Hz, 1H, CO–CH$_2$–C<u>H</u>), 6.02 (d, $J = 9.0$, 1H, CO–CH=C<u>H</u>), 6.40 (d, $J = 9.0$, 1H, CO–C<u>H</u>=CH), 7.13 (d, $J = 8.0$ Hz, 1H, Ar–H), 7.22 (d, $J = 8.0$ Hz, 1H, Ar–H), 7.49 (d, $J = 8.0$ Hz, 1H, Ar–H), 7.89 (d, $J = 8.0$ Hz, 1H, Ar–<u>H</u>), 9.84 (Ar–OH); ^{13}C NMR (100 MHz, $CDCl_3$) δ: 15.36 (CH_3), 36.28 (CH), 84.10, 92.52 (CH=CH), 118.20, 130.56, 134.22, 144.21, 156.03, 168.42 (Ar–C), 190.12 (C=O); MS (ES^+), *m/z* (%): 262.82 (100), $[M]^+$.

*3-(4-Methoxyphenyl)-8a-methyl-4a,5-dihydrobenzo-1,2,4-trioxin-6(8aH)-one (**3h**)*

UV spectrum (MeOH), λ_{max}, nm: 279.5; IR (KBr, cm^{-1}) υ: 2956.33, 2880.16 (C–H, CH_3), 1674.20 (C=O, conjugated), 1642.13, 1582.30, 1424.10 (C=C, aryl), 1152.82 (C–O), 878.41 (O–O); ^{1}H NMR (400 MHz, $CDCl_3$) δ: 1.19 (s, 3H, CH_3), 2.43 (d, $J = 4.0$ Hz, 2H, CO–C<u>H</u>$_2$–CH), 4.39 (s, 3H, OCH_3), 4.23 (d, $J = 4.0$ Hz, 1H, CO–CH$_2$–C<u>H</u>), 6.04 (d, $J = 10.0$, 1H, CO–CH=C<u>H</u>), 6.37 (d, $J = 10.0$, 1H, CO–C<u>H</u>=CH), 7.16 (d, $J = 7.0$ Hz, 1H, Ar–H), 7.28 (d, $J = 7.0$ Hz, 1H, Ar–H), 7.44 (d, $J = 8.0$ Hz, 1H, Ar–H), 7.82 (d, $J = 8.0$ Hz, 1H, Ar–<u>H</u>); ^{13}C NMR (100 MHz, $CDCl_3$) δ: 15.68 (CH_3), 28.67 (OCH_3), 38.40 (CH), 84.65, 92.28 (CH=CH), 118.18, 126.12, 132.17, 140.72, 152.32, 162.25 (Ar–C), 190.20 (C=O); MS (ES^+), *m/z* (%): 276.42 (100), $[M]^+$.

*3-(Furan-2-yl)-8a-methyl-4a,5-dihydrobenzo-1,2,4-trioxin-6(8aH)-one (**3i**)*

UV spectrum (MeOH), λ_{max}, nm: 219.5, 259.2; IR (KBr, cm^{-1}) υ: 2932.10, 2872.63 (C–H, CH_3), 1662.12 (C=O, conj.), 1128.00 (C–O), 882.12 (O–O); ^{1}H NMR (400 MHz, $CDCl_3$) δ: 1.18 (s, 3H, CH_3), 2.20 (d, $J = 3.0$ Hz, 2H, CO–C<u>H</u>$_2$–CH), 4.27 (d, $J = 3.0$ Hz, 1H, CO–CH$_2$–C<u>H</u>), 6.20 (d, $J = 9.0$, 1H, CO–CH=C<u>H</u>), 6.44 (d, $J = 9.0$, 1H, CO–C<u>H</u>=CH), 7.06 (d, $J = 8.0$ Hz, 1H, furan-2-yl-H$_3$), 7.10 (t, 1H, $J = 8.0$ Hz, furan-2-yl-H$_4$), 7.48 (d, 1H, $J = 9.0$ Hz, furan-2-yl); ^{13}C NMR (100 MHz, $CDCl_3$) δ: 15.10 (CH_3), 36.12 (CH), 86.52, 88.46 (CH=CH), 109.00,

114.26, 118.40, 122.35 (Ar–C, 1*H*-pyrrole-2-yl), 188.20 (C=O); MS (ES^+), *m/z* (%): 236.77 (100), $[M]^+$.

*3-(Pyridin-2-yl)-8a-methyl-4a,5-dihydrobenzo-1,2,4-trioxin-6(8aH)-one (**3j**)*

UV spectrum (MeOH), λ_{max}, nm: 262.5; IR (KBr, cm^{-1}) *υ*: 3023.22, 3010.23 (C–H, aryl), 2932, 2822.11 (C–H, CH_3), 1667.34 (C=O, conj.), 1481.36, 1450.25 (C=C, conj., aryl), 1154.20 (C–O), 872.13 (O–O); ^{1}H NMR (400 MHz, $CDCl_3$) *δ*: 1.26 (s, 3H, CH_3), 2.63 (d, $J = 4.0$ Hz, 2H, CO–C$\underline{H}_2$–CH), 4.32 (d, $J = 4.0$ Hz, 1H, CO–CH_2–C$\underline{H}$), 6.21 (d, $J = 8.0$, 1H, CO–CH=C$\underline{H}$), 6.40 (d, $J = 8.0$, 1H, CO–C$\underline{H}$=CH), 7.48 (d, $J = 8.0$ Hz, 1H, 4-pyridyl-$H_{2/6}$), 7.68 (d, $J = 8.0$ Hz, 1H, 4-pyridyl-$H_{3/5}$); ^{13}C NMR (100 MHz, $CDCl_3$) *δ*: 15.65 (CH_3), 34.12 (CH), 84.72, 92.68 (CH=CH), 116.20, 122.58, 128.34, 140.67 (Ar. C, 4-pyridyl), 188.42 (C=O); MS (ES^+), *m/z* (%): 247.03 (100), $[M]^+$.

Evaluation of antimalarial activity

Chemicals and parasite strains

All the synthesized compounds, **3a–j** were evaluated for in vitro antimalarial activity at multiple doses against CQ-sensitive (3D7) and CQ-resistant (RKL9) strains of *P. falciparum* using blood (erythrocytic) stage of parasite. The solvents and reagents used in the antimalarial study were of analytical grade and were procured from Sigma-Aldrich Corporation (USA) and HiMedia Lab. Pvt. Ltd. (Germany).

Assay procedure

The in vitro antimalarial activity screening was carried out by microculture Giemsa Stained slide method based on light microscopy. Schizont maturation inhibition assay technique was used for the quantitative assessment of parasitaemia and evaluation of drug sensitivity. The assay was conducted using the blood parasite of in vitro *P. falciparum* culture according to the previously reported methods (Trager and Jensen 1976; Lambros and Vanderberg 1976). Briefly, a continuous culture of *P. falciparum* strain was maintained *in vitro* in A^+ human red blood cells (RBCs) diluted to 5% hematocrit (HCT) in RPMI (Roswell Park Memorial Institute)-1640 medium supplemented with 25 mM HEPES [(N-2-hydroxyethylpiperazine-N-2-ethane sulfonic acid)] buffer, 1% D-glucose, 5.0% sodium bicarbonate, gentamycin (40 µg/mL), and 10% human AB^+ serum. Incubations were done at 37 °C and 5% CO_2 level in a modular incubator. The culture was passaged with fresh mixture of erythrocytes and complete RPMI medium for every day to maintain cell growth. D-sorbitol (5%) synchronized 1% ring stage parasitaemia in 5% HCT was used for the antimalarial assay using 96-well microtitre plate. A stock solution of 1.0 mg/mL of the test compound was prepared in dimethyl sulphoxide and subsequent dilutions were made with incomplete RPMI to obtain different concentrations (50, 25, 12.5, 6.25, 3.13, 1.56, 0.78, 0.39, and 0.19 µg/mL) of samples (test/standard) in duplicate. In addition, drug free negative control to assess the parasite growth and chloroquine diphosphate as positive control to assess the integrity of the assay were also maintained in duplicate in the microtitre plate. After 40 h of incubation at 37 °C the smears were prepared from each well (depending on the maturation of schizonts in negative control, ≥10%), stained with 3% Giemsa and examined under light microscope to ascertain drug sensitivity by assessing the level of parasitaemia i.e., the inhibition of parasite growth in terms of percent inhibition of schizonts' maturation (Rudrapal et al. 2013; Roy et al. 2013).

Observation and assessment of activity

Each test compound was assayed in duplicate and number of schizonts was counted against 200 asexual parasites per replica under light microscope. The number of schizonts count was also assessed in negative control maintained in duplicate in the microtitre plate. Mean number of schizonts for duplicate observations was calculated at each concentration of test/standard samples compounds. Test values were compared with the control values. The IC_{50} (concentration at which the inhibition of parasite growth represents 50%) values in µg/mL were also calculated using the NonLin *v*1.1 software (Kashyap et al. 2016). Test results were compared with the standard results of CQ.

In silico studies

Molecular docking study

Molecular modeling studies were carried out using Dell Precision work station T3400 running Intel Core2 Duo Processor, 4 GB RAM, 250 GB hard disk and NVidia Quodro FX 4500 graphics card. Two-dimensional (2D) structures of all compounds were built on Chemdraw Ultra 10.0 (Cambridge Soft Co., USA, 2010) and Marvin Sketch (ChemAxon LLC, Cambridge, USA, 2015) software. The 2D structures were later transformed into three-dimensional (3D) structures using the converter module of Biovia Discovery Studio (DS) *v* 4.5 (2015) software. All the conformations generated were then energetically minimized by a single step Steepest Descent method using CHARMM (Chemistry at HARvard Macromolecular Mechanics, Cambridge, USA) Force Field with 5000 iterations and a

minimum root mean square (RMS) gradient of 0.01 kcal/mol/Å (Singh et al. 2016).

The x-ray crystal structure of falcipain 2-E-64 (PDB id: 3BPF) was retrieved from the RCSB Protein Data Bank (http://www.rcsb.org/pdb/) and Chain A of the protein determined at a resolution of 2.9 Å was used in the study (Sashidhara et al. 2012a, b). Prior to docking, protein was prepared using protein preparation wizard tool of DS. Polar hydrogen atoms were added to the proteins and charges were assigned. All bound water molecules, other heteroatoms and ligands were excluded from the crystal structure as they were not significant for the proteins' function. Subsequently, the 3D structure of protein was optimized by energy minimization using CHARMM Force Field. It was done in two steps to remove the bad steric clashes using Steepest Descent and Conjugate Gradient methods for 5000 steps at RMS gradients of 0.01 and 0.05 kcal/mol/Å, respectively (Singh et al. 2016).

Molecular docking studies were carried out using Libdock program available in Biovia Discovery Studio (DS) *v* 4.5 (2015) software packages. After energy minimization, the Chain A of falcipain 2 protein was defined as a receptor and the binding site sphere was selected based on the ligand binding location of E-64. A receptor grid was thereby generated around the binding cavity (active sites) of protein by specifying the key amino acid residues (Cys 42, Gly 83, and His 174) (Sashidhara et al. 2012a, b). In DS, binding site sphere was set with a radius of 20 Å and *x*, *y*, *z* dimensions of −52.25, −4.46, −19.25, respectively. Flexible molecular docking was performed where the protein was held rigid while the ligands were allowed to be flexible during refinement. During docking, the falcipain 2-E-64 complex was imported and E-64 molecule (co-crystal ligand) was removed, and ligands were placed in the predicted binding site (grid box) and docking was performed using the Dock Ligands module of LibDock genetic algorithm program (Usha et al. 2014) of DS. All other docking and consequent scoring parameters used were kept at their default settings. The LibDock scores of the docked ligands were calculated. A number of dock poses were studied to know the best binding mode of receptor–ligand complex in terms of scoring function. The number of dock poses generated was 20 for each compound. All docked poses were scored, ranked and the best pose of each compound having the highest score was selected and it was later used for the receptor–ligand interaction analysis. Interaction of ligands with receptor was studied to know the best binding orientation of receptor–ligand complex having maximum LibDock score. Binding modes of the best pose for each compound was also analyzed with the help of 3D receptor–ligand complex. Different non-bonding interactions (hydrogen bonding and hydrophobic) were also analyzed with the help of 2D diagram of docked receptor–ligand complexes. Receptor–ligand interaction study out for better understanding the molecular interactions between the binding site residues of receptor molecule and complimentary groups/atoms of ligands involved in interactions.

Molecular properties calculation and drug-likeness studies

In silico calculations of the molecular properties and drug-likeness parameters for all compounds, **3a–j** were performed based on theoretical approaches to identify the compounds which violate the optimum requirements for drug-likeness. Molecular properties (molecular weight, Log*P* value, number of hydrogen bond acceptor(s), number of hydrogen bond donor(s), total polar surface area (TPSA)) incorporated in Lipinski's rule of five (Lipinski et al. 1997) and other physicochemical parameters like aqueous solubility (LogS), molar refractivity and molar volume were calculated using Calculation of Molecular Properties module of Biovia DS *v* 4.5 software. The number of rotatable bonds was predicted using Molsoft Online software (http://www.molsoft.com), and non-violation of drug-likeness and drug-likeness score were calculated using Molinspiration online software (http://www.molindpiration.com).

ADMET prediction

ADME-toxicity (ADMET) for all the target compounds was calculated in silico using ADMET descriptor module of Biovia DS *v* 4.5 software. Six mathematical models (aqueous solubility, blood-brain barrier (BBB) penetration, cytochrome P450 2D6 inhibition, hepatotoxicity, human intestinal absorption, and plasma protein binding) were used to quantitatively predict properties related to ADMET characteristics or pharmacokinetics of molecules (Alam and Khan 2014). These properties influence oral bioavailability, cell permeation, and metabolism of drug molecules.

Results and discussion

Design of compounds

Rationale behind the design strategy involved selection of 1,2,4-trioxane ring system as the parent peroxide scaffold considering the pharmacodynamic importance of 1,2,4-trioxane component for antimalarial activity of ART and related endoperoxides. Our study was aimed at developing 1,2,4-trioxane derivatives as newer synthetic peroxide-based antimalarial agents having comparatively simpler molecular framework than conventional antimalarial drug molecules with activity against resistant malaria parasites. Target compounds (Fig. 2) were designed with diverse

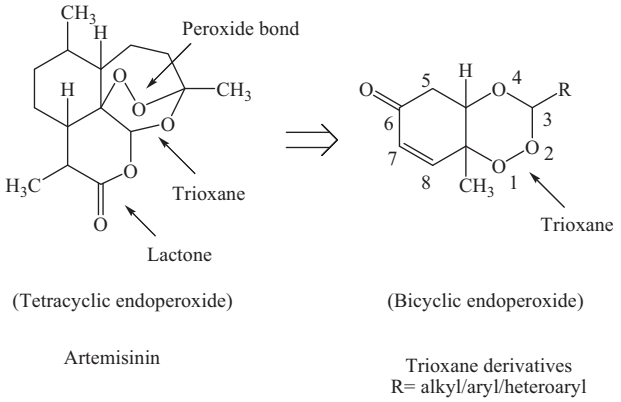

Fig. 2 Design of 1,2,4-trioxane derivatives

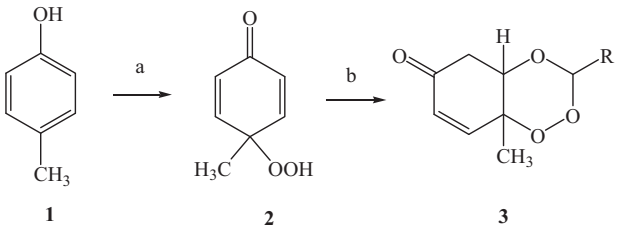

Fig. 3 Scheme of synthesis of target compounds, **3a–j**. Reagents and conditions: **a** Oxone, $NaHCO_3/CH_3CN/H_2O$, rt; **b** RCHO, 40–50 °C, 8–12 h, CH_2Cl_2, PTSA

substitution patterns (alkyl/aryl/heteroaryl groups) at C-3 position of the 1,2,4-trioxane structural scaffold, based on the molecular manipulation approach of drug design with due consideration to all structure and property parameters that are relevant to biological activity. The 1,2,4-trioxane ring system was considered as the basic requirement for the antimalarial activity and substitutions with groups/moieties having electronic property of (s) was the main motif behind the design task.

Chemistry

In our study, new series of 1,2,4-trioxane derivatives were synthesized and evaluated in vitro for their antimalarial activity. Substitutions with different aliphatic, aromatic, and heteroaromatic groups at the C-3 position of 1,2,4-trioxane ring system afforded target trioxane derivatives obtained as single drug conjugates. The standard reaction procedure (Rubush et al. 2012) involving a facile synthetic route depicted in Fig. 3 was employed for the preparation of 1,2,4-trioxane derivatives. The oxidative dearomatization of *p*-cresol, **1** with oxone first yielded the intermediate compound, *p*-peroxyquinol, **2** which was later allowed to react with different aldehydes (aliphatic/aromatic/heteroaromatic) in presence of an acid catalyst called PTSA, to obtain desired trioxane deivatives, **3a–j**. The first step of reaction was a [4 + 2] cycloaddition between electron rich *p*-alkyl phenol and $^1O_2$ (singlet oxygen) generated in situ in the reaction system from oxone, which gave *p*-peroxyquinol intermediate through a 1,4-endoperoxide i.e., peroxyhemiacetal. Subsequent desymmetrization of *p*-peroxyquinol after reaction with aldehydes with the help of PTSA catalyst yielded different trioxane derivatives (Fig. 4) (Carreno et al. 2006). The progress of reactions was monitored by the silica gel-G thin-layer chromatography (TLC) and the spots were visualized by iodine vapors. The purity of the synthesized compounds was ascertained by melting point determinations and silica gel G TLC. All the compounds were obtained in good yields with high purity. The physicochemical details of synthesized compounds are summarized in Table 1.

The spectral (UV, IR, ^{1}HNMR, ^{13}CNMR, mass) data depicted in the experimental section are in close agreement with the structures of synthesized compounds. In UV spectra (in methanol), λ_{max} values were observed at the range of 202.5–279.5 which was due to the presence of chromophoric trioxane ring system along with alkyl/aryl/heteroaryl substituents at the C-3 position of the parent scaffold. IR spectral data showed absorption frequencies characteristic to specific functional groups and/or bonds present in the structure of synthesized compounds. The appearance of a broad peak at 3174.10, 3182.67, and 3186.13 cm^{-1} confirmed the presence of phenolic –OH group in the structure of **3e**, **3f**, and **3g**, respectively. The carbonyl (C=O) group was assigned with a strong and sharp absorption band in the region of 1682.45–1643.20 cm^{-1} for all the synthesized compounds. Distinguished C–O stretching band was appeared in the range of 1078.23–1128.00 cm^{-1}. A weak absorption band observed at 898.20–832.119 cm^{-1} was due to O–O stretching. The presence of aliphatic C–H (CH_3/CH), aromatic C–H (CH=C) and aromatic C=C groups in the structure of synthesized compounds were also confirmed by characteristic peaks as depicted in the experimental section.

^{1}HNMR spectra exhibited resonance signals with chemical shift (δ, ppm) values characteristic to various structural protons which concorded the anticipated structure of synthesized compounds. A singlet for three protons of CH_3 group of the trioxane ring system was observed in the range of 1.12–1.26 ppm. Depending on the nature of the substituent at C-3 position of the trioxane ring, distinct δ values were also observed with expected splitting patterns (doublets, triplets or multiplets) and coupling constant (J) values. A broad singlet at 9.52, 9.64, and 9.84 ppm was observed due to aromatic OH proton for compounds, **3e**, **3f**, and **3g**, respectively. Distinct singlet due to three protons of the OCH_3 group was appeared at 4.39 ppm for compound **3h**. Aromatic protons including heteroaryl substituents were appeared in the range of 7.14–7.89 ppm. Aliphatic methyl

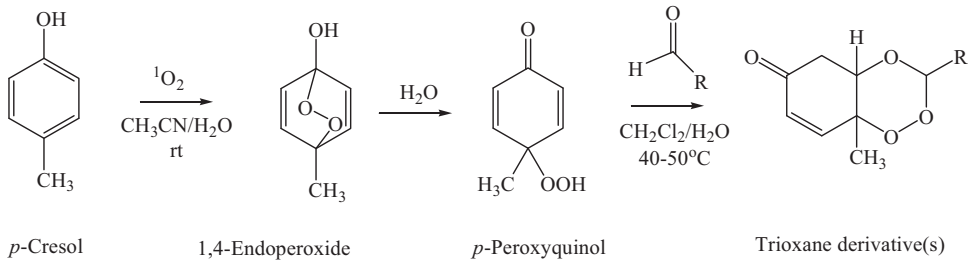

Fig. 4 Reaction mechanism of synthesis of 1,2,4-trioxane derivative(s)

Table 1 Physicochemical data

Comp.	R	MF	Color (state)	% Yield	MP (°C)	R_f[a]
3a	H	$C_8H_{10}O_4$	Colorless (solid)	84	102–104	0.67
3b	Methyl	$C_9H_{12}O_4$	Colorless (solid)	78	108–110	0.72
3c	Isopropyl	$C_{11}H_{16}O_4$	Colorless (solid)	68	118–121	0.76
3d	Phenyl	$C_{14}H_{14}O_4$	Colorless (solid)	74	122–124	0.72
3e	3-Hydroxyphenyl	$C_{14}H_{14}O_5$	Brown (semi-solid)	68	–	0.68
3f	3,4-Dihydroxyphenyl	$C_{14}H_{14}O_6$	Brown (semi-solid)	70	–	0.66
3g	4-Hydroxyphenyl	$C_{14}H_{14}O_5$	Colorless (solid)	72	120–124	0.76
3h	4-Methoxyphenyl	$C_{15}H_{16}O_5$	Pale yellow (solid)	74	128–130	0.72
3i	Furan-2-yl	$C_{12}H_{12}O_5$	Brown (semi-solid)	65	–	0.65
3j	Pyridine-2-yl	$C_{13}H_{13}O_4$	Brown (semi-solid)	68	–	0.69

[a] Diethyl ether:EtOAc:acetic acid (1:3:0.5)

(CH_3) and methine (CH) protons were observed in multiplet pattern (doublet or triplet) at δ values in the downfield region for compounds **3b** and **3c**, as depicted in experimental section (Silverstein and Webster 2005).

In ^{13}C NMR spectra, distinguished resonance signal due to the carbonyl (>C=O) carbon was appeared in the range of 188.12–191.34 ppm. Aromatic/heteroaromatic carbons were appeared at 109.00–168.42 ppm. Characteristic downfield signals for aliphatic carbons were observed for CH_3 (14.20–18.24 ppm), OCH_3 (28.67 ppm, **3h**) and CH (34.12–46.39 ppm) groups. Olefinic (CH=CH) carbons were also assigned and depicted in the experimental section. The mass spectra of **3a–j** exhibited prominent molecular ion peaks, $[M]^+$ which finally confirmed the structure of compounds with the anticipated mass corresponding to their respective molecular formula.

Antimalarial activity

Results of in vitro antimalarial activity (Table 2) revealed that all the synthesized compounds (**3a–j**) showed activity against both CQ-sensitive (3D7) and CQ-resistant (RKL9) strains of *P. falciparum* in a dose dependant manner with IC_{50} values ranging from 0.391 to 0.652 and 0.827 to 2.240 µg/mL against CQ-sensitive and CQ-resistant strains of *P. falciparum*, respectively. Out of ten tested compounds, five compounds (**3e–j**) exhibited good activity as compared to rest of the analogs, with better activity profile against resistant strain than the sensitive one. The IC_{50} value of the best compound (**3g**) was found to be 0.391 and 0.837 µg/mL against sensitive strain and resistant strain of *P. falciparum*, respectively. Results of tested compounds were comparable with that of the standard drug, CQ (IC_{50} = 0.044 and 0.205 µg/mL against sensitive and resistant strain

Table 2 In vitro antimalarial activity data

Comp.	IC_{50} in µg/mL ± SD[a]	
	Pf 3D7	*Pf* RKL9
3a	0.652 ± 0.002	2.167 ± 0.004
3b	0.648 ± 0.003	2.198 ± 0.002
3c	0.642 ± 0.005	2.240 ± 0.002
3d	0.638 ± 0.006	2.018 ± 0.004
3e	0.476 ± 0.003	1.925 ± 0.003
3f	0.403 ± 0.002	1.222 ± 0.002
3g	0.391 ± 0.002	0.827 ± 0.002
3h	0.478 ± 0.004	1.973 ± 0.003
3i	0.492 ± 0.003	1.989 ± 0.005
3j	0.478 ± 0.005	1.958 ± 0.004
CQ[b]	0.044 ± 0.006	0.205 ± 0.006

[a] Calculated using *NonLin v1.1* software, mean ± SD (standard deviation) of two replicate observations (counted against 200 asexual cells per replicate)

[b] CQ—Chloroquine used as standard reference drug

of *P. falciparum*, respectively). Figure 5 shows photographs of the effect of the most active compound, **3g** against both CQ-sensitive (3D7) and CQ-resistant (RKL9) strains of *P. falciparum*.

Results indicate different structural substitutions such as non-bulky alkyl and bulky aryl/heteroaryl groups at C-3 position of the ring system modulates the antimalarial efficacy of prepared 1,2,4-trioxane derivatives. Some degree of variations in activity among synthesized analogs might be due to diverse structural substitutions. A brief structure–activity relationship (SAR) study can be depicted as follows: no substitution or non-bulky small alkyl substituents like methyl, or isopropyl moieties are of considerable importance for the activity. Substitution with bulky aryl moieties also contributes good antimalarial potency to a similar or greater extent as compared to alkyl substituted analogs. Compounds with phenyl substitutions sufficiently retains the activity, whereas, 3-hydroxyphenyl, 3,4-dihydroxyphenyl, 4-methoxyphenyl substitution considerably increases the activity. Substitution with 4-hydroxyphenyl significantly increases the activity. With bulky heteroaryl moieties like furan-2-yl and pyridine-2-yl substitutions also potentiate the activity. It is also clear that compounds with five membered heterocyclic rings like furan-2-yl are less important for the activity than six membered heteroaryl systems like pyridyl ring. Upon critical analysis of SAR, the most notable point found is that substitutions electron releasing groups (alkyl, aryl rings substituted with electron releasing groups) considerably increases the activity. More illustratively, phenyl substituent with electron releasing (OH, OCH_3 etc.) groups significantly increases the activity (Fig. 6). Substitutions of electron releasing groups at *para* or both at *meta* and *para* have greater contributing effects than *meta* substitutions. Di-substitution (3,4-dihydroxy, compound **3f**) is less important for the activity than mono *meta*-substitution (3-hydroxyphenyl, compound **3e**), and *para*-substitution (4-hydroxyphenyl, compound **3g**). The findings of our present study are also consistent with earlier report (Sashidhara et al. 2012a, b) on trioxane-based compounds shows excellent antiparasitic activity upon incorporation of an aryl group. It is seen that bulkiness of substituents is important for the activity. However, aryl substitution seems to be more important than alkyl or heteroaryl substitution. It is important to note here that besides bulkiness of substituents, lipophilicity (hydrophobicity) and ionization potential (basicity) of the molecule are also considered to play a crucial role for the activity. The lipophilicity (log*P*) is inevitable for permeation of parasitic membrane and basicity (pKa) is required for accumulation of trioxane molecule in the acidic food vacuole of parasites.

Literature report that 1,2,4-trioxane structure lacking the lactone ring play an important role for the antimalarial activity, but 1,2,4-trioxane ring alone is insufficient for optimal antimalarial potency as compared to ART and its semi-synthetic analogs (Liu et al. 2011). The reductive cleavage of the peroxide bond in vivo by haem [Fe(II)] (released during hemoglobin degradation process in parasitized RBC) and subsequent production of cytotoxic carbon-centered radicals target cell proteins/enzymes and destroys parasites (Meshnick 2002; Cumming et al. 1996; Paul et al. 2004).

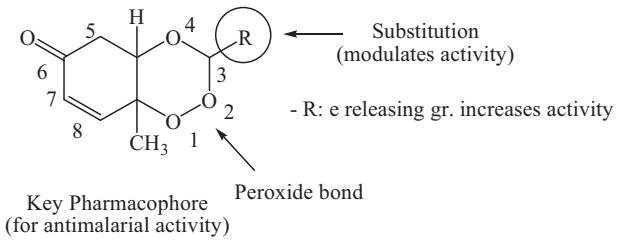

Fig. 6 Effect of substitutions on antimalarial activity of 1,2,4-trioxane derivatives

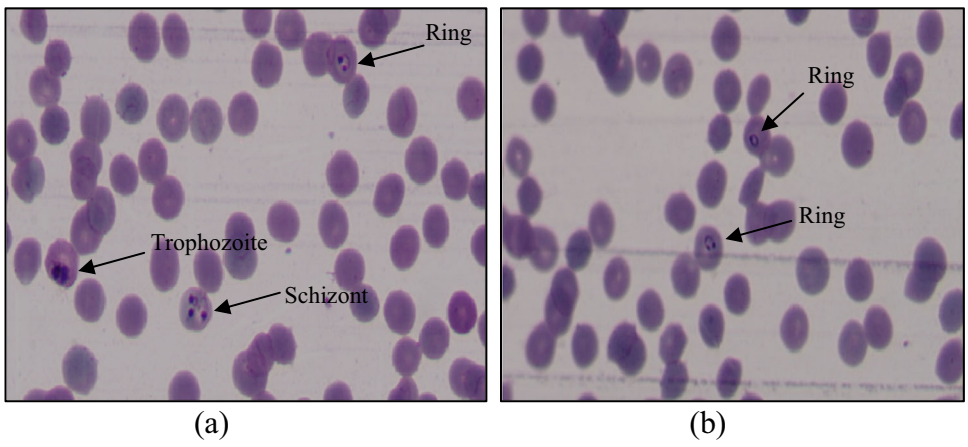

Fig. 5 Photographs showing in vitro antimalarial activity of the most active compound, **3g** against **a** CQ-sensitive 3D7 and **b** CQ-resistant RKL9 strains of *P. falciparum*

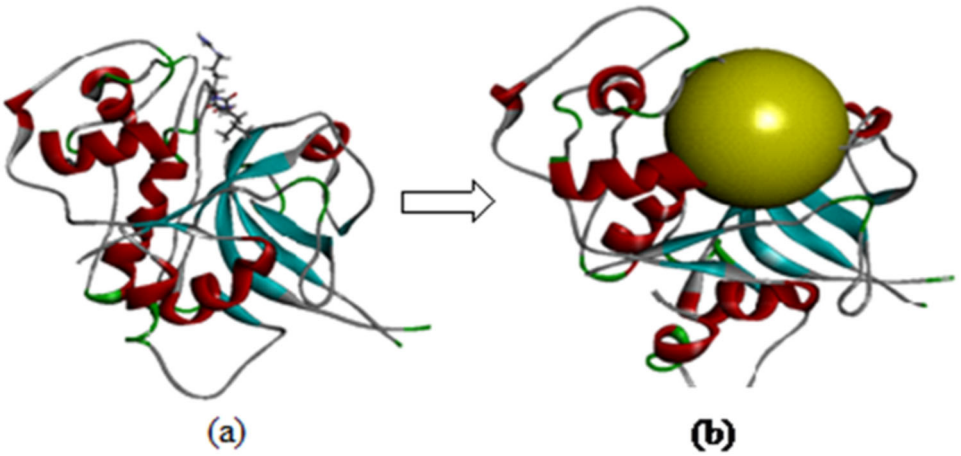

Fig. 7 **a** Optimized co-crystal structure of falcipain 2 (Chain A)-E-64, **b** receptor grid for docking

Docking simulations

Plasmodium cysteine protease falcipain 2 enzyme plays an essential role in the degradation of host hemoglobin into smaller peptides which takes place in the acidic food vacuole of *P. falciparum*. Recent literature (Oliveria et al. 2013) claims that endoperoxide antimalarials have potential to inhibit falcipain 2 enzyme and therefore, drug targeting of this particular enzyme would be an attractive avenue in the design and development of new antimalarial drugs. Accordingly, a molecular docking study was performed for all newly designed compounds **3a–j**, using the falcipain 2 enzyme as receptor molecule.

The protein model used for docking study was validated as follows: the three dimensional crystal structure of falcipain 2 co-crystallized with the inhibitor *trans*-epoxysuccinyl-*L*-leucylamido-(4-guanidino) butane (E-64) with active site (receptor grid model) as defined by Cys 42, Gln 36, and His 174 residues was optimized and used for the study. The co-crystal structure of falcipain 2-E-64 (PDB: 3BPF) and the receptor grid model used for docking study are represented in Fig. 7. Co-crystallized ligand, E-64 was re-docked using flexible docking simulations (LibDock program of DS) into the original structure of the target protein, falcipain-2 by non-covalent docking procedure. For this study, docking parameters were set to the software's default values. E-64 was successfully re-docked to the predicted active sites of falcipain 2 with an acceptable RMSD value of 1.124 Å. Further, in order to reproduce an experimentally observed ligand-binding mode, the co-crystallized ligand, E-64 (a selective falcipain 2 inhibitor) was used as reference ligand. Results confirmed experimental binding conformations of E-64 in the binding pocket of receptor molecule. The binding modes and ligand–protein interaction diagrams obtained in re-docking of E-64 are shown in Fig. 8a.

Docking results revealed that LibDock program successfully docked all 1,2,4-trioxane derivatives into the binding pocket of falcipain 2 enzyme. All compounds which were active in in vitro test could bind with the active site of falcipain-2 with high docking score (LibDock) and binding affinities in the range of 75.682–125.232. The LibDock scores are summarized in Table 3. All trioxane derivatives except **3a**, **3b**, and **3c** exhibited more binding affinity (higher dock scores) than the co-crystal ligand, E-64 (Libdock score = 100.364). Five compounds which showed more potency in in vitro study also ranked top in docking study with LibDock scores of 120.143, 122.807, 125.232, 114.923, 101.911, and 118.049 for **3a**, **3b**, **3c**, **3d**, **3e**, **3f**, and **3g**, respectively. It is important to note here that docking results are generally analyzed by a statistical scoring function which converts interacting energy (binding energy) into numerical values called as the docking score, and therefore docking score is nothing but an expression of binding energy (Lionta et al. 2004). Binding energy (ΔG) includes the sum of all non-bonded interactions including hydrogen bonding, hydrophobic, and Vander Walls between protein residues and bound ligand (Kitchen et al. 2004). LibDock score is useful to assess the antimalarial activity of ligands as *P. falciparum* falcipain 2 inhibitors. Docking scores of compounds supported the results of in vitro antmalarial activity of synthesized 1,2,4-trioxane derivatives.

Protein–ligand docking was performed to generate the bioactive binding poses of designed inhibitors in the active site of falcipain 2 enzyme. LibDock is a high throughput docking algorithm that finds various conformations of the ligands in the protein active site based on polar interaction sites (hotspots) (Usha et al. 2014). The 3D poses of bound ligands were visualized which revealed that the best orientation of the ligand relative to the receptor as well as the conformation of the ligand and receptor (best fit of

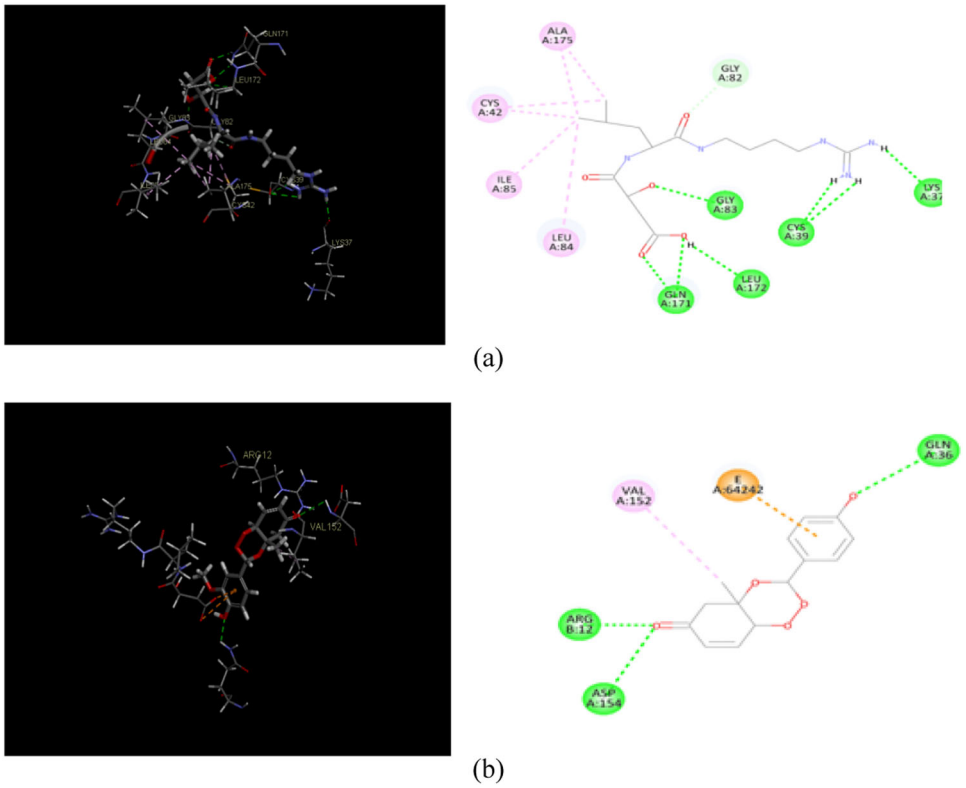

Fig. 8 **a** Redocked conformer (pose) of co-crystal ligand, E-64 in the active site of the protein falcipain 2 (left) and 2D representation of the binding interaction (right); **b** Binding mode (left) and 2D receptor-ligand interaction diagram (right) of compound **3g** at binding pocket of falcipain 2

Table 3 LibDock scores and no. of H-bonds

Comp.	LibDock score	No. of H-bond(s)
3a	75.682	2
3b	77.062	2
3c	97.656	2
3d	107.807	4
3e	120.143	4
3f	122.807	4
3g	125.232	4
3h	114.923	6
3i	101.911	3
3j	118.049	5
E-64[a]	100.364	7

[a] Co-crystal ligand

ligand in the receptor molecule). Analysis of 2D diagram indicated that various non-bonded interactions mainly polar hydrogen bonding interactions were involved between binding site residues (active site amino acids) and ligand moieties/atoms. Table 3 also depicts the number of hydrogen bonds (H-bonds) for all docked compounds. Higher the number of hydrogen bonds, higher is the binding affinity. Apart from hydrogen bonding interactions other non-bonded interactions like hydrophobic bonding were also observed.

Table 4 revealed the hydrogen bonding interactions of five most potent compounds (**3e–j**) with active site residues such as Asn 38, Asp 154, Asp 170, Arg 12, Gln 36, Glu 15, Glu 138, Gly 13, Gly 15, Gly 169, Cys 39, and His 19. Compound **3g** which showed the highest antimalarial activity among the series, could bind the active sites of falcipain-2 mainly by hydrogen bonding interactions. The 3D binding modes and 2D interaction diagrams of the most potent compounds, **3g** are shown in Fig. 8b. Compound **3g** formed four strong hydrogen bonds with residues like Arg 12 (O··H··O), Cys 39 (O··H··O), Gln 36 (O··H··O) and Asp 154 (O··H··O) with bonding distances of 1.686, 2.038, 2.745, and 2.934 A^{o}, respectively. Analysis of best docking pose of **3g** revealed that the trioxane scaffold was oriented in the binding cavity (active site residues) of falcipain 2 receptor molecule. In 2D diagram, the trioxane moiety could occupy the binding sites of falcipain-2 through strong H-bonding interactions along with hydrophobic interactions. Such interactions afforded good stability between receptor molecule and ligand. Trioxane moiety interacted with multiple amino acid residues such as Arg 12, Gln 36, and Asp 154 residues interacted with the 4-hydroxyphenyl in compound **3g**, respectively. Strong H-bonding interactions between C=O group of the trioxane and amino acid residues were also observed. The OH groups were involved for H-bonding interactions from the substituent moieties for compound **3g**. Further analysis of docking interactions, it

Table 4 Details of hydrogen bonding ligands and receptor molecule for five most active compounds

Comp.	H-bond(s)	H-binding ligand		H-binding receptor			H-bond distance (A°)
		Element	Type	Residue	Element	Type	
3e	4	O	A	ARG 12	H	D	1.467
		H	D	CYS 39	O	A	2.123
		H	A	ASN 38	O	D	2.056
		O	A	GLU 15	H	D	2.078
3f	4	H	A	GLY 13	O	D	1.458
		H	D	CYS 39	O	A	2.032
		O	A	HIS 19	H	D	2.490
		H	A	ASP 154	O	D	2.123
3g	4	O	A	ARG 12	H	D	1.686
		H	D	CYS 39	O	A	2.038
		O	A	GLN 36	H	D	2.745
		O	A	ASP 154	H	D	2.934
3h	6	O	A	ASP 170	H	D	2.005
		O	A	ARG 12	H	D	3.074
		O	A	GLY 169	H	D	2.826
		O	A	HIS 19	H	D	2.438
		H	D	GLY 13	O	A	3.056
		H	D	GLU 15	O	A	2.995
3j	6	O	A	ARG 12	H	D	2.999
		N	A	ARG 12	H	D	2.866
		O	A	HIS 19	H	D	2.474
		H	D	GLY 15	O	A	2.827
		H	D	GLU 15	O	A	2.885
		O	A	ARG 12	H	D	2.999

was found that trioxane ring played a crucial role in protein–ligand binding. Substituents increased binding strength by forming additional H-bonds that facilitated much stronger interaction of ligands with the receptor (falcipain-2 protein) molecule with optimum binding affinity to achieve desired antimalarial activity.

Docking is generally used to find the best binding orientation of small molecules bound to their target protein molecules in order to predict the binding affinity and thereby biological activity of the small molecules. Hence, docking plays an important role in the rational drug design. To evaluate the ligand–receptor interactions the best pose of receptor–ligand complex should possess the lowest free energy (binding energy) which differ from experimentally observed other structure and estimate the binding affinity. Search algorithm is used to generate different poses of the ligand within the active site of molecules, orientations of particular conformations of the molecule in the binding site. Scoring function is used to identify the most likely pose for an individual ligand to assign a priority order to a set of diverse ligands docked to the same protein and hence estimate binding affinity. Using scoring function, one can predict the binding conformation of a ligand in its receptor and the affinity between the ligand and the receptor with the correct poses of ligands in the binding pocket of a protein (Lionta et al. 2004; Usha et al. 2014; Nikam et al. 2015; Sapre et al. 2008).

Molecular properties and drug-likeness

The results of predicted Lipinski's parameters and other drug-likeness properties of the synthesized compounds, **3a–j** are depicted in Table 5. Results revealed that all the compounds possessed good drug-like properties based on Lipinski's rule of five with additional parameters such as molar solubility (MS), molar volume (MV), molar refractivity (MR), and number of rotable bonds (nRotB). All compounds obeyed Lipinski's rule of five and Veber rule. Lipinski rule of five is a rule to evaluate drug likeness to determine if a chemical compound has a certain pharmacological or biological activity to make it an orally active drug (Khoshneviszadeh et al. 2016). According to Lipinski's rule, compounds are more likely to be drug-like and orally bioavailable if they obey the following criteria: Log$P_{o/w}$ (octanol/water partition coefficient) ≤ 5, MW (molecular weight) ≤ 500, HBA (hydrogen bond

Table 5 Calculated molecular properties and drug-likeness parameters

Comp.	Lipinski's parameters						MS	MR	MV (A^3)	nRotB	DL score
	MW	LogP	nHBA	nHBD	TPSA (A^2)	nViolations					
3a	170.16	0.11	4	0	44.76	0	−0.57	40.78	187.56	0	−1.09
3b	184.18	0.45	4	0	44.76	0	−1.00	45.58	202.89	0	−0.83
3c	212.24	1.28	4	0	44.76	0	−1.64	54.46	236.53	1	−0.85
3d	246.26	2.17	4	0	44.76	0	−2.68	65.27	255.79	1	−0.82
3e	262.26	1.79	5	1	64.99	0	−2.21	66.97	268.63	1	−0.17
3f	278.26	2.12	4	0	44.76	0	−2.42	68.79	262.02	1	−0.72
3g	262.26	1.79	5	1	64.99	0	−2.21	66.97	268.63	1	−0.17
3h	276.29	2.26	5	0	53.99	0	−2.81	71.74	287.64	2	−0.54
3i	236.23	1.32	4	0	57.90	0	−2.08	57.68	241.85	1	−0.70
3j	247.25	2.39	4	1	60.55	0	−2.21	71.87	296.39	1	−1.24

MW molecular weight, *LogP* log of octanol/water partition coefficient, *nHBA* no. of hydrogen bond accepror(s), *nHBD* no. of hydrogen bond donor (s), *TPSA* total polar surface area, *nViolations* no. of rule of five violations, *MS* molar aqueous solubility, *MR* molar refractivity, *MV* molar volume, *nRotB* no. of rotable bonds, *DL* drug-likeness

acceptors) ≤ 10 and HBD (hydrogen bond donors) ≤ 5 (Sharma et al. 2016). To further substantiate Veber et al. stated that compounds with ≤10 rotatable bonds and TPSA of ≤140 A^2 are more likely to show membrane permeability and good bioavailability (Khoshneviszadeh et al. 2016; Faidallah et al. 2016). Lipinski rule of five is considered predictive for oral bioavailability; however, 16% of oral drugs violate at least one of the criteria and 6% fail in two or more (Khoshneviszadeh et al. 2016). In our study, compounds did not violate Lipinski rule of five parameters. Poor absorption or permeation of a ligand is more likely if a drug-like molecule have more than one of five rule violations. Values of LogP, MW, and TPSA indicated that compounds possessed good membrane permeability and oral bioavailability, whereas, nRotb bonds suggested that compounds had good intestinal availability. MS data indicated good bioavailability of compounds if given by oral route. MV and MR values were also found in permissible range which indicated good oral bioavailaility for all the compounds. Hydrophobicity, membrane permeability and bioavailability are dependent on molecule's MW, LogP, MS, HBA, and HBD. Molecules violating more than one of these rules fail to exhibit optimum bioavailability. Sufficient water solubility is also important for optimal bioavailability of drugs. Number of rotable bonds is important for molecular conformational studies (i.e., stereoselectivity of drug molecules) for optimal binding with the receptor molecule. Reduced molecular flexibility, as measured by the number of rotatable bonds, and polar surface area or total hydrogen bond count (sum of donors and acceptors) are some important predictors of good oral bioavailability, independent of molecular weight (Sharma et al. 2016). Further, TPSA, MV, and MR are also useful parameters for drug's transport and biodistribution (Sharma et al. 2016). The drug score combines drug-likeness, lipophilicity, solubility, molecular weight, and the risk of toxicity into a single numerical value that can be used to predict a global value for each compound as a potential new drug candidate (Kashyap et al. 2016). Drug-likeness score were obtained in the range of −1.24 and −0.17. Even though compounds exhibited negative drug-likeness values, scores were in acceptable range and indicated that compounds possessed potential as new drug candidates. The overall analysis of drug-likeness studies strongly suggested that newly designed 1,2,4-trioxane derivatives possessed good drug-likeness behavior favorable for optimal membrane permeability, transport and bioavailability, and eventual interaction with the receptor molecule.

Since all newly designed compounds showed favorable drug-like properties a reasonable correlation can be drawn between their calculated drug-like properties and in vitro antimalarial activity profile. $\text{Log}P_{o/w}$ is a direct indicator of lipophilicity of drug substances. Higher the value of logP, better the biological membrane permeability. It is inevitable for a molecule to have sufficient lipophilicity which is required for its optimal bioavailability and biological action. Hydrogen bond acceptor and donor groups are of paramount importance required to achieve optimal drug action. PSA is also closely related to the hydrogen bonding potential of a drug molecule. Practically, a compound with all drug-like properties in the desired range appears to exhibit high levels of therapeutic potency. Good drug-like properties and activity are complementary, and hence balanced attention to both properties and bioactivity could suitably transform a ligand to a good drug lead (Grover et al. 2014; Debnath and Ganguly 2016; Kerns and Di 2008; Kashid et al. 2013). Better antimalarial activity of the top six compounds, **3a–j** might probably due to their sufficient

Table 6 Theoretical ADMET parameters

Comp.	Aqueous solubility	BBB penetration	CYP P450 2D6 inhibition	Hepatotoxicity	Intestinal absorption	PP binding
3a	3	2	False	True	0	False
3b	3	2	False	True	0	False
3c	3	1	False	True	0	False
3d	2	1	False	False	0	True
3e	3	2	False	False	0	False
3f	3	1	False	False	0	False
3g	3	2	False	False	0	False
3h	2	2	False	False	0	True
3i	3	2	False	True	0	True
3j	3	2	False	False	0	False

Aqueous solubility: 3-good, 2-low; Blood brain barrier (BBB) penetration: 3-low, 2-medium, 1-moderate; Cytochrome (CYP) P450 2D6 inhibition: false-non-inhibitor; Hepatotoxicity: true-toxic, false-non-toxic; Intestinal absorption: 0-good; Plasma protein (PP) binding: true-highly bounded, false-poorly bounded

lipophilicity along with balanced polar properties likes HBD, HBA groups, rotable bonds, and PSA. They collectively determine membrane permeability as well as transport property of drug molecule. Because of having optimal lipophilicity compound readily penetrated parasite's cell membrane that led to attain an intracellular concentration for desired antimalarial activity.

ADMET prediction

The ADMET values of newly designed 1,2,4-trioxane derivatives presented in Table 6 were found in acceptable range with favorable ADMET properties. All the compounds were predicted to have good intestinal absorption and non-inhibitors of cytochrome P450 2D6 (CYP2D6) with medium to moderate BBB penetration. BBB penetration is mandatory for the drug to be used in the treatment of cerebral malaria. The CYP2D6 enzyme is one of the important enzymes involved in drug metabolism. The aqueous solubility prediction (defined in water at 25 °C) indicated that most of the compounds were soluble in water. The predictive hepatotoxicity was observed for a few compounds among three series. Some of the compounds were found to be highly bound with plasma protein, while some were poorly bound with plasma protein.

Conclusion

Since newly reported 1,2,4-trioxane derivatives have significant in vitro antimalarial effectiveness, further studies are required for the evaluation of their toxicity, antimalarial efficacy and pharmacokinetics in animal models. Structure–activity relationship study helped us to understand the importance of the 1,2,4-trioxane core system along with various substitution patterns on the overall antimalarial activity of 1,2,4-trioxane analogs. Pharmacodynamic significance and unique structural simplicity of trioxane molecules highlighted their potential to be used as future antimalarial agents. In silico studies also confirms that newer 1,2,4-trioxane derivatives developed as single drug conjugates possess target specific action against *P. falciparum* falcipain 2 receptor with well defined physicochemical, pharmacokinetic and toxicity properties. All these results yielded valuable information for optimization of 1,2,4-trioxane-based compounds to be developed as novel as falcipain 2 inhibitors with the help of structure-based drug design approach. Further, QSAR and pharmacokinetic-based optimization studies are also required to develop new antimalarial drug candidates from present series of 1,2,4-trioxane lead molecules.

Acknowledgements Authors are thankful to Bioinformatics Infrastructure Facility, Center for Biotechnology and Bioinformatics, Dibrugarh University, Dibrugarh, Assam (India) for carrying out in silico studies. Authors are also thankful to SAIF, Panjab University, Chandigarh for providing spectral data of synthesized compounds.

Compliance with ethical standards

Conflict of interest The authors declare that they have no competing interests.

References

Alam S, Khan F (2014) QSAR and docking studies on xanthone derivatives for anticancer activity targeting DNAtopoisomerase IIα. Drug Des Dev Ther 8:183–195

Balint GA (2001) Artemisinin and its derivatives: an important new class of antimalarial agents. Pharmacol Ther 90:261–265

Carreno MC, Gonzalez-Lopez M, Urbano A (2006) Oxidative dearomatization of para-alkyl phenols into para-peroxyquinols and *para*-Quinols mediated by oxone as a source of singlet oxygen. Angew Chem Int Ed 45:2737–2741

Cumming JN, Ploypradith P, Posner GH (1996) Antimalarial activity of artemisinin (*qinghaosu*) and related trioxanes: mechanism(s) of action. Adv Pharmacol 37:253–297

Debnath B, Ganguly S (2016) Synthesis, biological evaluation, in silico docking, and virtual ADME studies of 2-[2-oxo-3-(arylimino)indolin-1-yl]-*N*-arylacetamides as potent anti-breast cancer agents. Monatsh Chem 147:565–574

Faidallah HM, Al-Mohammadi MM, Alamry KA, Khan KA (2016) Synthesis and biological evaluation of fluoropyrazolesulfonylurea and thiourea derivatives as possible antidiabetic agents. J Enzyme Inhib Med Chem 31(sup1):157–163

Garner P, Graves PM (2005) The benefits of artemisinin combination therapy for malaria extend beyond the individual patient. PLoS Med 2(4):e105

Geleta G, Ketema T (2016) Severe malaria associated with *P. falciparum* and *P. vivax* among children in Pawe Hospital, Northwest Ethiopia. Malar Res Treat 6:1–7

Gogoi J, Chetia D, Kumawat MK, Rudrapal M (2016) Synthesis and antimalarial activity evaluation of some mannich bases of tetraoxane-phenol conjugate. Indian J Pharm Edu Res 50 (4):591–597

Grover J, Kumar V, Singh V, Khemraj B, Sobhia ME, Jachak SM (2014) Synthesis, biological evaluation, molecular docking and theoretical evaluation of ADMET properties of nepodin and chrysophanol derivatives as potential cyclooxygenase (COX-1, COX-2) inhibitors. Eur J Med Chem 80:47–56

Kashid AM, Dube PN, Alkutkar PG, Bothara KG, Mokale SN, Dhawale SS (2013) Synthesis, biological screening and ADME prediction of benzylindole derivatives as novel anti-HIV-1, antifungal and anti-bacterial agents. Med Chem Res 22:4633–4640

Kashyap A, Chetia D, Rudrapal M (2016) Synthesis, antimalarial activity evaluation and drug-likeness study of some new Quinoline-Lawsone Hybrids. Indian J Pharm Sci 78(6):892–911

Kerns EH, Di L (2008) Drug-like properties: concepts, structure design and methods from ADME to toxicity optimization. Academic Press, New York, p 6–14

Khoshneviszadeh M, Shahraki O, Khoshneviszadeh M, Foroumadi A, Firuzi O, Edraki N, Nadri H, Moradi A, Shafiee A, Miri R (2016) Structure-based design, synthesis, molecular docking study and biological evaluation of 1,2,4-triazine derivatives acting as COX/15-LOX inhibitors with anti-oxidant activities. Enzyme Inhib Med Chem 31(6):1602–1611

Kitchen DB, Decornez H, Furr JR, Bajorath J (2004) Docking and scoring in virtual screening for drug discovery: methods and applications. Nat Rev 3:936–849

Kyle DE, Teja-Isavadharm P, Li Q, Leo K (1998) Pharmacokinetics and pharmacodynamics of qinghaosu derivatives: how do they impact on the choice of drug and the dosage regimens? Med Trop 58:38–44

Lambros C, Vanderberg JP (1976) Synchronization of *Plasmodium falciparum* erythrocytic stages in culture. J Parasitol 65:418–420

Lionta E, Spyrou G, Vassilatis DK, Cournia Z (2004) Structure-based virtual screening for drug discovery: principles, applications and recent advances. Curr Top Med Chem 14:1923–1938

Lipinski CA, Lombardo F, Dominy BW, Feeney PJ (1997) Experimental and computational approaches to estimate solubility and permeability in drug discovery and development settings. Adv Drug Deliv Rev 23:3–26

Liu Y, Cui K, Lu W, Luo W, Wang J, Huang J, Guo C (2011) Synthesis and antimalarial activity of novel dihydro-artemisinin derivatives. Molecule 16:4527–4538

Meshnick SR (2002) Artemisinin: mechanisms of action, resistance and toxicity. Int J Parasitol 32:1655–1660

Nikam MD, Mahajan PS, Damale MG et al. (2015) Synthesis, molecular docking and biological evaluation of some novel tetrazolo [1,5-*a*]quinoline incorporated pyrazoline and isooxazoline derivatives. Med Chem Res 24:3372–3386

Oliveria R, Newton AS, Guedes RC, Miranda D, Amewa RK, Srivastava A, Gut J, Rosenthal PJ, O'Neill PM, Ward S, Lopes F, Moreira R (2013) An endoperoxide-based hybrid approach to deliver Falcipain inhibitors inside malaria parasites. Chem Med Chem 8:1528–1536

Pandey S, Agarwal P, Srivastava K, RajaKumar S, Puri SK, Verma P, Saxena JK, Sharma A, Lal J, Chauhan PMS (2013) Synthesis and bioevaluation of novel 4-aminoquinoline-tetrazole derivatives as potent antimalarial agents. Eur J Med Chem 66:69–81

Park VK, O'Neill PM, Maggs JL (1998) Safety assessment of peroxide antimalarials: clinical and chemical perspectives. Br J Clin Pharmacol 46:521–529

Paul M, O'Neill PM, Posner GH (2004) A medicinal chemistry perspective on Artemisinin and related endoperoxides. J Med Chem 47(12):2945–2964

Roy S, Chetia D, Rudrapal M, Prakash A (2013) Synthesis and antimalarial activity study of some new Mannich bases of 7-chloro-4-aminoquinoline. Med Chem 9:379–383

Rubush DM, Morges MA, Rose BJ, Thamm DH, Rovis T (2012) An asymmetric synthesis of 1,2,4-trioxane anticancer agents via desymmetrization of Peroxyquinols through a Brønsted acid catalysis cascade. J Am Chem Soc 134:13554–13557

Rudrapal M, Chetia D (2016) Endoperoxide antimalarials: development, structural diversity and pharmacodynamic aspects with reference to 1,2,4-trioxane-based structural scaffold. Drug Des Dev Ther 10:3575–3590

Rudrapal M, Chetia D, Prakash A (2013) Synthesis, antimalarial- and antibacterial activity evaluation of some new 4-aminoquinoline derivatives. Med Chem Res 22:3703–3711

Sapre NS, Gupta S, Pancholi N, Sapre N (2008) Molecular docking studies on tetrahydroimidazo-[4,5,1-jk] [1,4]-benzodiazepinone (TIBO) derivatives as HIV-1 NNRT inhibitors. J Comput Aided Mol Des 22:69–80

Sashidhara KV, Avula SR, Palnati GR, Singh SV, Srivastava K, Puri SK, Saxena JK (2012a) Synthesis and in vitro evaluation of new chloroquine-chalcone hybrids against chloroquine-resistant strain of *Plasmodium falciparum*. Bioorg Med Chem 22:5455–5459

Sashidhara KV, Kumar K, Dodda RP, Krishna NN, Agarwal P, Srivastava K, Puri SK (2012b) Coumarin–trioxane hybrids: Synthesis and evaluation as a new class of antimalarial scaffolds. Bioorg Med Chem 22:3926–3930

Sharma D, Chetia D, Rudrapal M (2016) Design, synthesis and antimalarial activity of some new 2-hydroxy-1,4-naphthoquinone-4-hydroxyaniline Hybrid Mannich Bases. Asian J Chem 28 (4):782–788

Shukla S, Srivastava RS, Shrivastava SK, Sodhi A, Kumar P (2013) Synthesis, cytotoxic evaluation, docking and in silico pharmacokinetic prediction of 4-arylideneamino/cycloalkylidineamino 1, 2- naphthoquinone thiosemicarbazones. J Enzyme Inhib Med Chem 28(6):1192–1198

Silverstein RM, Webster FX (2005) Spectrometric identification of organic compounds. Wiley Inc, New York, p 205–213

Singh J, Kumar M, Mansuri R, Sahoo GS, Deep A (2016) Inhibitor designing, virtual screening, and docking studies for methyltransferase: A potential target against dengue virus. J Pharm Bioallied Sci 8(3):188–194

Singh S, Srivastava P (2015) Molecular docking studies of myricetin and its analogs against human PDK-1 kinase as candidate drugs for cancer. Comput Mol Biosci 5:20–33

Singh SP, Konwar BK (2012) Molecular docking studies of quercetin and its analogs against human inducible nitric oxide synthase. SpringerPlus 1:69

Tang Y, Dong Y, Vennerstrom JL (2004) Synthetic peroxides as antimalarials. Med Res Rev 24:425–448

Trager W, Jensen JB (1976) Human malaria parasites in continuous culture. Science 193:673–675

Usha T, Middha SK, Goyal AK, Karthik M, Manoj DA, Faizan S, Goyal P, Prashanth HP, Pande V (2014) Molecular docking studies of anti-cancerous candidates in *Hippophae rhamnoides* and *Hippophae salicifolia*. J Biomed Res 28(5):406–415

White NJ (1994) Clinical pharmacokinetics and pharmacodynamics of artemisinin and derivatives. Trans R Soc Trop Med Hyg 88: S41–S43

White NJ (1997) Assessment of the pharmacodynamic properties of antimalarial drugs in vivo. Antimicrob Agents Chemother 41:1413–1422

World Malaria Report (2016) World Health Organization, Geneva